Chemistry A European Journal

Chemistry Europe
European Chemical Societies Publishing

Title: Facile Synthesis of Azahelicenes and Diaza[8]circulenes through the Intramolecular Scholl Reaction

Authors: Chihiro Maeda, Shuichi Nomoto, Koki Akiyama, Takayuki Tanaka, and Tadashi Ema

To be cited as: *Chem. Eur. J.* 10.1002/chem.202102269

Link to VoR: https://doi.org/10.1002/chem.202102269

WILEY-VCH

Facile Synthesis of Azahelicenes and Diaza[8]circulenes through the Intramolecular Scholl Reaction

Chihiro Maeda,*[a] Shuichi Nomoto,[a] Koki Akiyama,[a] Takayuki Tanaka,[b] and Tadashi Ema*[a]

[a] Dr. C. Maeda, S. Nomoto, K. Akiyama, Prof. T. Ema
Division of Applied Chemistry, Graduate School of Natural Science and Technology, Okayama University,
Tsushima, Okayama 700-8530, Japan
E-mail: cmaeda@okayama-u.ac.jp
ema@cc.okayama-u.ac.jp

[b] Dr. T. Tanaka
Department of Chemistry, Graduate School of Science, Kyoto University,
Sakyo-ku, Kyoto 606-8502, Japan

Supporting information for this article is given via a link at the end of the document.

Abstract: Carbazole-based aza[7]helicenes and hetero[9]helicenes were successfully obtained via the intramolecular Scholl reaction of 3,6-bis(biphenyl-2-yl)carbazole congeners, while the reaction of 3,6-bis(naphthylphenyl)-appended carbazole gave a triple helicene via an unexpected simultaneous double aryl rearrangement. DFT calculations suggested that the rearrangement proceeded via an arenium cation intermediate. In addition, the reaction of methoxy-appended substrate gave an azahepta[8]circulene via the concurrent C–C bond formation. These helical dyes showed circularly polarized luminescence. The azahepta[8]circulene was further transformed into deeply saddle-distorted dibenzodiaza[8]circulenes as the first example of its solution-based synthesis and unambiguous structural determination.

Introduction

Circulene derivatives and congeners have been recognized as unique polycyclic aromatic hydrocarbons (PAHs), and their structural and electronic properties have attracted considerable attention.[1–6] [6]Circulene consisting of six *ortho*-fused benzene rings adopts a planar structure, while larger circulenes often adopt nonplanar saddle-shaped structures to reduce the strain. Among the circulenes, hetero[8]circulenes, which have one or more fused heterole rings around the cyclooctatetraene (COT) skeleton instead of fused benzene rings, have been actively investigated owing to their optelectronic properties and possible antiaromatic contribution from the central COT rings (Figure 1a). Pristine [8]circulene adopts a saddle-shaped structure,[3] while four or eight heterole-containing [8]circulenes adopt nearly planar structures.[4,5] Diheterole-based [8]circulenes occupies an important position to exploit deeper understanding in their properties and to create a new class of highly strained PAHs. However, their intrinsic high strain energies have hampered their synthesis in the solution state and only on-surface synthesis of the π-extended diaza[8]circulene has recently been achieved by Ito and co-workers.[6]

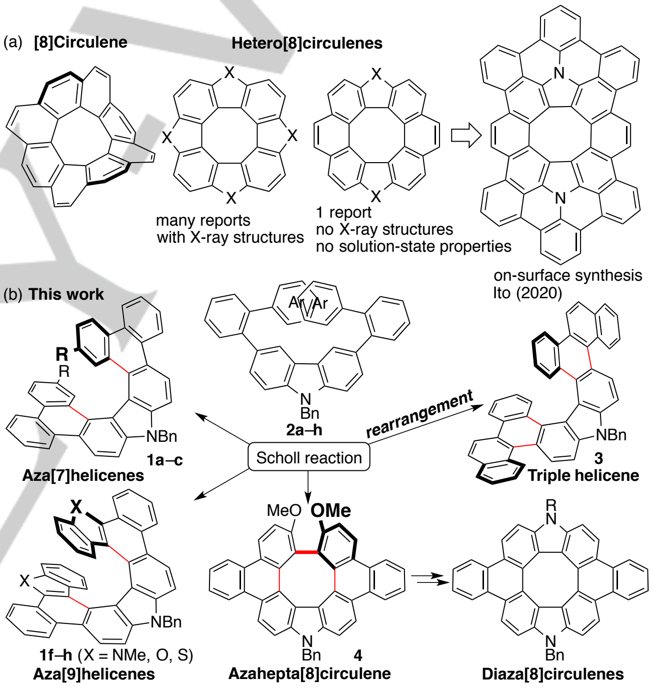

Figure 1. (a) Structures of [8]circulenes. (b) Synthesis of azahelicenes and diaza[8]circulenes in this work.

As another strained motif, helicenes have also received considerable attention during the last decade, and their structural and chiroptical properties have been actively studied.[7–10] We have explored the synthesis and chiroptical properties of chiral carbazole-based BODIPY analogues, and recently reported the synthesis of azahelicene-fused boron complex, where the novel carbazole-based azahelicene was developed via the short step synthesis.[11] In this paper, we synthesized a series of carbazole-based azahelicenes via the intramolecular Scholl reaction of 3,6-bis(biphenyl-2-yl)carbazole congeners **2a**–**h** to investigate their chiroptical properties (Figure 1b). Aza[7]helicenes **1a**–**c** and aza[9]helicenes **1f**–**h** were successfully obtained, while triple helicene **3** was produced from naphthyl-appended **2e** via a double aryl rearrangement. In addition, azahepta[8]circulene **4** was formed from **2d**.[12] We envisioned that **4** would serve as a useful intermediate for the synthesis of diaza[8]circulenes. Fortunately, we succeeded in the transformation of **4** into dibenzodiaza[8]circulenes and their unambiguous structural determination by X-ray diffraction analysis for the first time. Here, we report the synthesis, structures, and photophysical properties of the azahelicenes and aza[8]circulenes.

Results and Discussion

The $FeCl_3$-mediated intramolecular Scholl reaction of *N*-benzyl-3,6-bis(biphenyl-2-yl)carbazole (**2a**) gave azahelicene **1a** (Scheme 1). Similarly, azahelicenes **1b** and **1c** bearing methyl and *tert*-butyl groups were obtained in 95% and 42% yields, respectively.[13] Interestingly, the reaction of methoxy-substituted **2d** gave azahepta[8]circulene **4** via the concurrent aromatic coupling,[14,15] and the reaction of naphthyl-appended **2e** gave triple helicene **3** via an unexpected double aryl rearrangement.[16] **4** was characterized by NMR and mass spectroscopy, while **3** was elucidated by the X-ray diffraction analysis (Figure 2c). The X-ray crystal structure of **3** revealed the aza[7]helicene moiety and two [4]helicene moieties all of which adopted the same helicities. Furthermore, we conducted the reaction of **2f–h** with benzoheterole frameworks, which gave hetero[9]helicenes **1f–h**. **1h** was successively oxidized by mCPBA to **1i** with sulfonyl groups. The structures of **1b**, **1c**, **3**, and **1h** were confirmed by the X-ray diffraction analysis, which revealed the helical structures (Figure 2). The torsion angles of the carbazole moieties (C1-C2-C3-C4) increase as the size of the substituents increase, while that in **1h** was relatively small probably because of the stacking of the benzothiophene moieties. The enantiomers of helicenes were successfully separated by passing through a chiral column, and their absolute configurations were deduced by TD-DFT calculations (Supporting Information).[17]

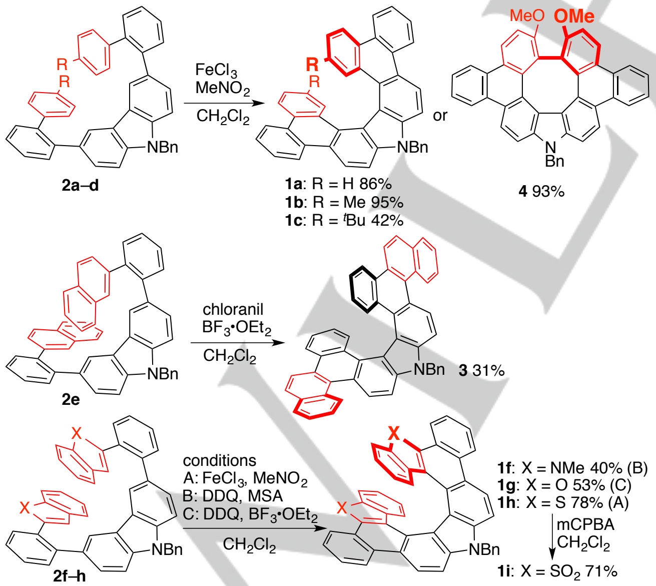

Scheme 1. Synthesis of azahelicenes.

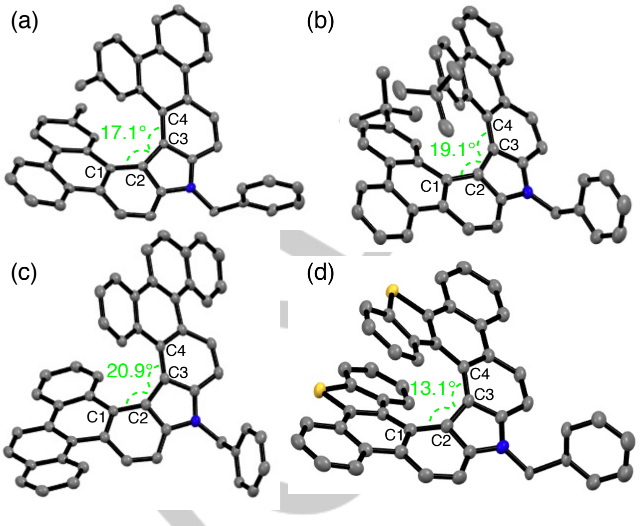

Figure 2. X-ray crystal structures of (a) **1b**, (b) **1c**, (c) **3**, and (d) **1h**. Hydrogen atoms and solvent molecules are omitted for clarity. The torsion angles of the carbazole moieties (C1-C2-C3-C4) are shown.

DFT calculations were performed to reveal the reaction mechanism of the rearrangement from **2e** to **3** at the (U)B3LYP/6-31G(d) level using SMD solvation effect of dichloromethane (Scheme 2 and S10 in Supporting Information). 3-[2-(Naphthalen-2-yl)phenyl]carbazole (**R**) was used as a model compound. We calculated two pathways from **R** to the helicenes (**A5** and **A8**) via the arenium cation and radical cation intermediates according to the literatures.[10j,16] First, the arenium cation pathway is proposed as follows (Scheme 2). Protonation of **R** at the 2-position of the naphthalene moiety gives **A1**.[18] C–C bond formation between the 3-position of the carbazole moiety and the 1-position of the naphthalene moiety provides **A2** with the bond length of 1.63 Å. Oxidation and deprotonation of **A2** affords **A3**, followed by the 1,2-phenyl shift to **A4**. The C–C bond lengths linked between the carbazole moiety and the naphthalene moiety in **A3** and **A4** are 1.55 Å and 1.46 Å, respectively, indicating relatively tight bonds at these stages. Finally, deprotonation of **A4** affords [5]helicene **A5** as a rearrangement product. On the other hand, C–C bond formation of **A1** at the 4-position of the carbazole moiety gives rise to **A6**. The oxidation and deprotonation of **A6** gives **A7** which is transformed into [6]helicene **A8**. The transition state energy from **A1** to **A2** and **A6** is 4.1 and 4.7 kcal/mol, respectively.[19] The kinetically favored formation of **A2** over **A6** as well as the large stabilization from **A2** into **A3** might promote the rearrangement to **A5** via the arenium cation pathway. Next, another possible pathway via the radical cation intermediate is proposed as follows (Scheme S10 in Supporting Information). The oxidation of **R** gives rise to a radical cation species **R1**. C–C bond formation of **R1** at the 3-position of the carbazole moiety forms spiro-fused adduct **R2**. The subsequent release of hydrogen radical gives **R3**, equivalent to **A3**. The 1,2-aryl shift of the phenyl group and the deprotonation provide [5]helicene **A5**. On the other hand, C–C bond formation of **R1** at the 4-position of the carbazole moiety forms 3,4-fused adduct **R4**. The subsequent release of hydrogen radical and proton gives [6]helicene **A8**. The transition state energy from **R1** to **R2** and **R4** is 27.2 and 24.9 kcal/mol, respectively, and the rearrangement via the radical cation pathway is considered to be disfavored. In the present study,

10.1002/chem.202102269

therefore, rearrangement via the arenium cation intermediate is considered to be dominant from the result of the calculations.

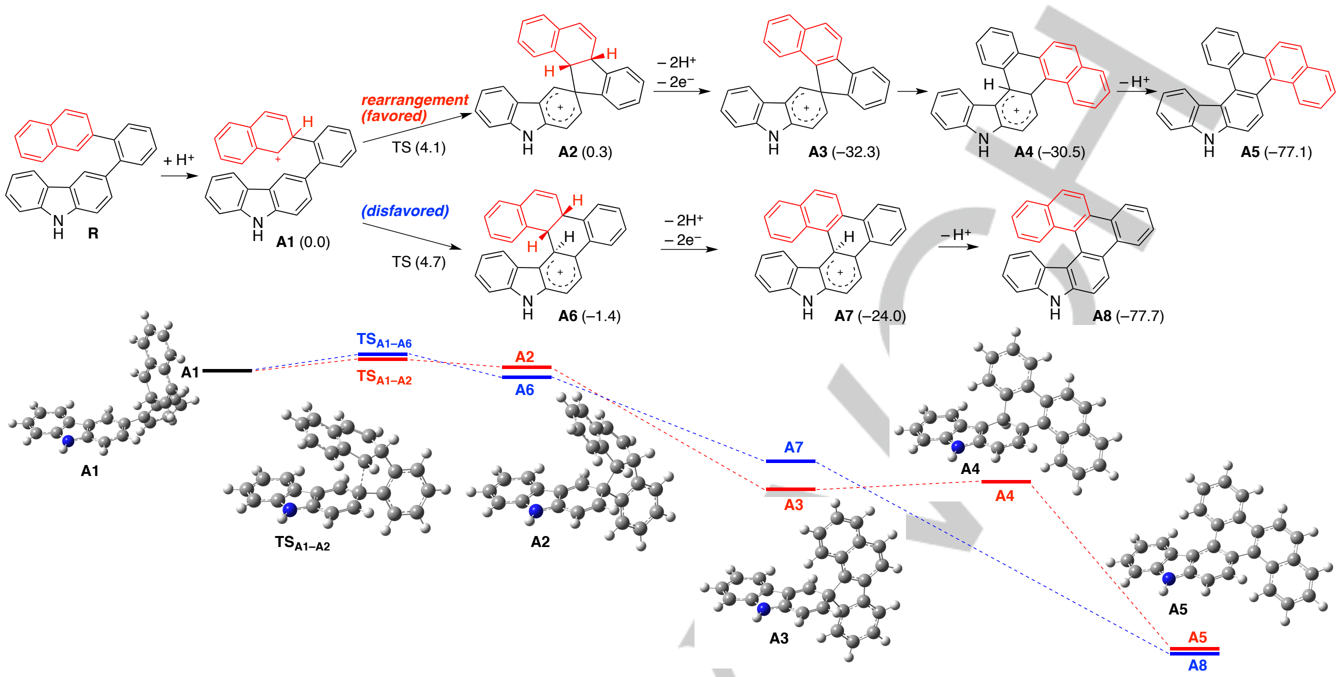

Scheme 2. Proposed reaction mechanism of the rearrangement from 3-[2-(naphthalen-2-yl)phenyl]carbazole (**R**) to helicene **A5** via arenium cation intermediates. The values in parenthesis are relative energies in kcal/mol. Potential energy profiles and selected optimized structures are shown. An energy gap between chloranil and tetrachlorohydroquinone is included in **A3** and **A7**, while that between [chloranil·H]⁻ and tetrachlorohydroquinone is included in **A5** and **A8**.

Chiroptical properties of the optically pure helicenes were investigated (Figure 3 and Table 1). All the helical dyes showed absorption at 250–450 nm and fluorescence at 400–550 nm with the fluorescence quantum yields of 0.08–0.31, and the Cotton effects and CPL signals were observed at the regions. The CD and CPL spectra of **1a**–**c** are similar, while the g_{abs} and g_{lum} values slightly increase with an increase of sizes of the substituents, and **1c** recorded the maximum $|g_{\mathrm{lum}}|$ of 0.0035. On the other hand, the Cotton effects and CPL intensities of azahepta[8]circulene **4** and triple helicene **3** were much weaker. The chiroptical properties of hetero[9]helicenes **1f**–**i** changed upon the replacement of the hetero atoms. (*P*)-Enantiomers of **1f**–**i** similarly showed the positive Cotton effects at 300 nm. For the longest wavelength regions, however, (*P*)-**1g**–**i** showed the negative Cotton effects, while (*P*)-**1f** showed the positive Cotton effect. The sign of CPL is consistent with the sign of the Cotton effects, suggesting that excited-state structures are similar to the ground-state structures.

Electrochemical properties were investigated by cyclic voltammetry. The oxidation potentials of **1b** and **1c** with alkyl substituents were 0.65 V and 0.66 V, respectively, which were slightly lower than that of **1a** (0.68 V). For hetero[9]helicenes, **1g** and **1h** showed one oxidation wave at 0.59 V and 0.61 V, respectively, while **1f** showed two oxidation waves at 0.22 and 0.60 V. The low first oxidation potential of **1f** might be ascribed to the fused carbazole trimer structure.

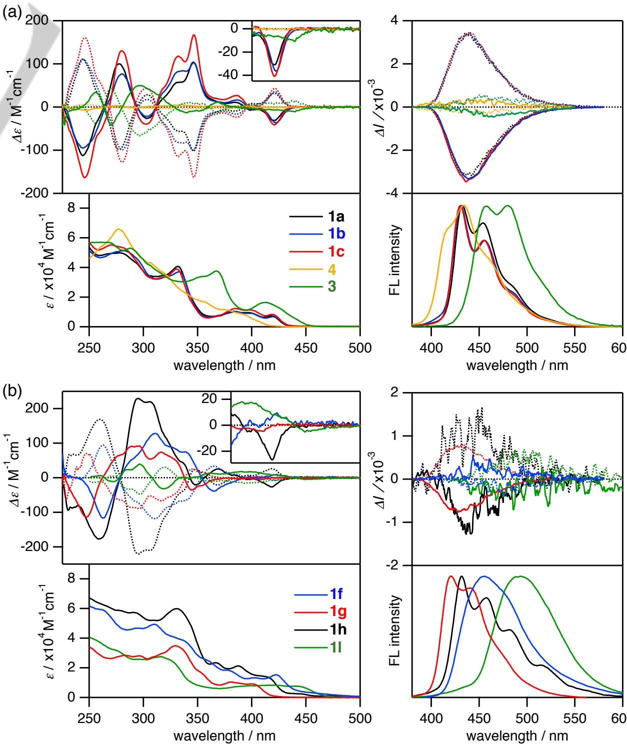

Figure 3. Chiroptical spectra in CH_2Cl_2. (a) **1a**–**c**, **3**, and **4**, and (b) **1f**–**i** (For CD and CPL, solid line: (*P*)-enantiomer, dotted line: (*M*)-enantiomer). Insets show the enlarged CD spectra of (*P*)-enantiomers.

Table 1. Chiroptical results in CH_2Cl_2.

compd	λ_A [nm]	g_{abs} [10^{-3}][a]	λ_F [nm][b]	Φ_F	g_{lum} [10^{-3}][b,c]
(*P*)-**1a**	418	–4.9	432, 454	0.28	–3.2
(*P*)-**1b**	419	–5.9	432, 455	0.27	–3.4
(*P*)-**1c**	419	–5.4	432, 456	0.31	–3.5
(*P*)-**4**	418[d]	+0.23	435	0.17	+0.25
(*P*)-**3**	422	–3.2	458, 480	0.10	–0.39
(*P*)-**1f**	412	+0.45	456	0.24	+0.29
(*P*)-**1g**	401	–0.92	420, 441	0.30	–0.72
(*P*)-**1h**	414[d]	–1.6	432, 457	0.08	–1.1
(*P*)-**1i**	440	–0.73	493	0.10	–0.26

[a] $g_{abs} = \Delta\varepsilon/\varepsilon$ at the maximum wavelength of the longest Cotton effects. [b] Excited at λ = 320 nm. [c] $g_{lum} = 2(I_L-I_R)/(I_L+I_R)$. Average values at $\lambda_F \pm 10$ nm. [d] Shoulder.

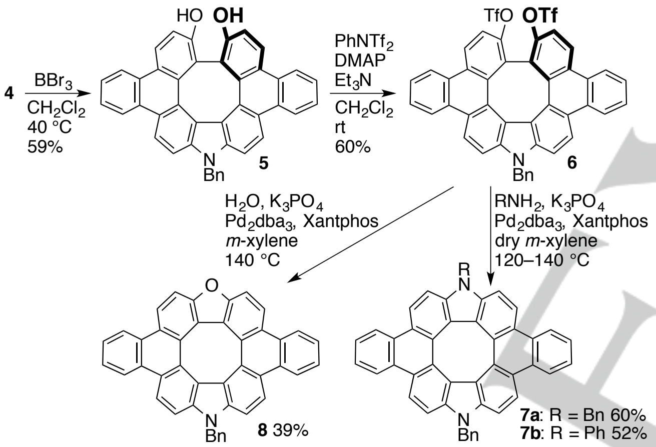

Scheme 3. Synthesis of dibenzohetero[8]circulenes.

We expected that azahepta[8]circulene **4** might be transformed into diaza[8]circulenes (Scheme 3).[20] Demethylation of **4** with BBr_3 gave dihydroxy-substituted **5**, which was converted into **5** with triflate groups. X-ray diffraction analysis of **6** revealed the structure of highly deformed azahepta[8]circulene framework (Figure 4a). To our delight, double amination reaction of **6** with benzylamine under palladium catalysis successfully provided dibenzodiaza[8]circulene **7a**. The reaction with aniline similarly provided the corresponding diaza[8]circulene **7b**. During the investigation of the amination reaction, azaoxa[8]circulene **8** was found to be obtained under the wet conditions.[8b] **8** was obtained in 39% yield in the presence of water under the amine-free conditions. The structure of **7a** was confirmed by the X-ray diffraction analysis, revealing the saddle-shaped diaza[8]circulene framework as the first example of diheterole-based [8]circulenes (Figure 4b). The mean plane deviation of the dibenzoazahepta[8]circulene moiety of **6** and the dibenzodiaza[8]circulene moiety of **7a** are 0.78 and 0.90 Å, respectively, indicating the distorted π-framework. The C–C bond lengths of the COT moiety are relatively long (1.44 and 1.47 Å) and are arranged alternately. The longer C–C bond lengths of the COT moiety indicate negligible 8π antiaromatic contribution, being analogous to previously reported hetero[8]circulenes. Consistently, the nucleus-independent chemical shift (NICS) value at the central position of the COT moiety of **7a** is calculated to be +9.10 ppm, that is ascribable to the induced paratropicity arising from the surrounding polycyclic aromatics.

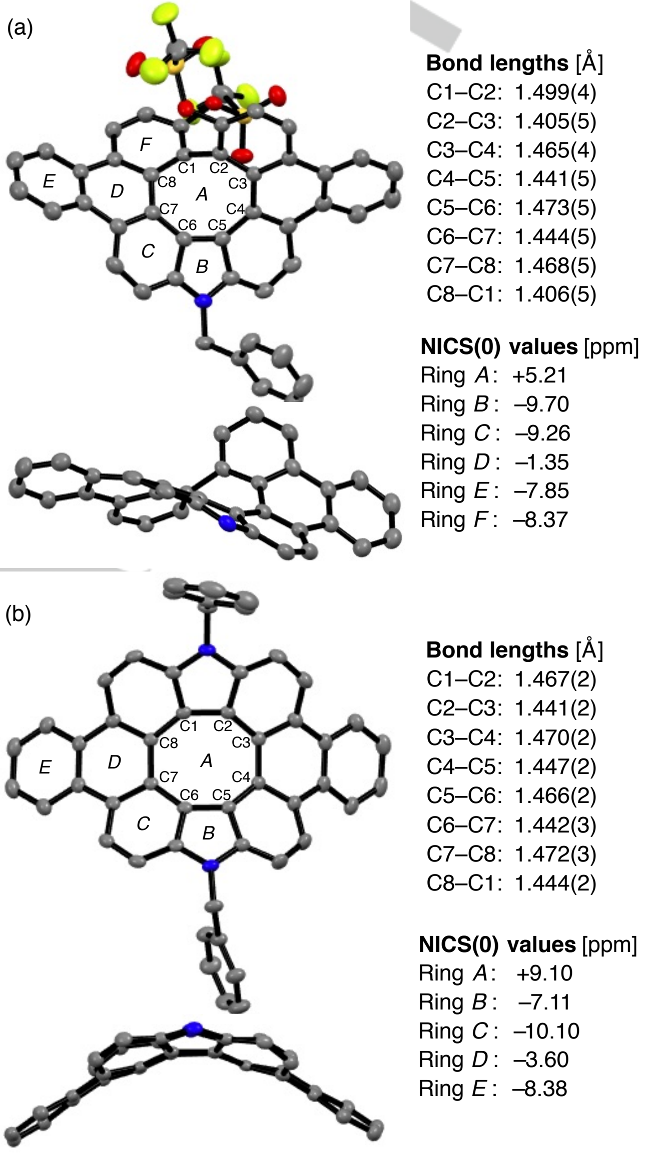

Figure 4. X-ray crystal structures of (a) **6** and (b) **7a**. Hydrogen atoms, solvent molecules, and peripheral substituents in the side views are omitted for clarity.

The UV/vis absorption and fluorescence spectra of **7a**, **7b**, and **8** are shown in Figure 5. The hetero[8]circulenes showed two main absorption bands at 250–350 nm and 350–500 nm, and the latter band of **7a** was assigned as the transition from the HOMO or HOMO–3 to the LUMO (Supporting Information). These molecular orbitals are based on a carbazole framework, and the allowed transitions are peculiar to aza[8]circulenes (Figure 6). The spectra of **7a** and **7b** are quite similar, while that of **8** is blue-shifted. As compared to the delocalized HOMO of **7a** (state 172), **8** showed the localized HOMO at the carbazole moiety (state 148), and the stabilized HOMO seems to contribute to the blue-shifted absorption. They showed fluorescence at 500–650 nm with the fluorescence quantum yields of less than 0.02. The broad fluorescence is different from tetraaza[8]circulenes probably due to the flexible framework in this system, and the benzo-fused moieties might accelerate vibration energy relaxation. Consequently, the diaza[8]circulenes have electronic states and flexible structure similar to tetraaza[8]circulenes and pristine [8]circulenes, respectively.

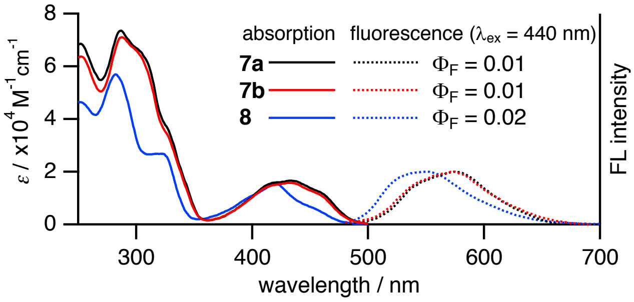

Figure 5. UV/vis absorption and fluorescence spectra in CH_2Cl_2.

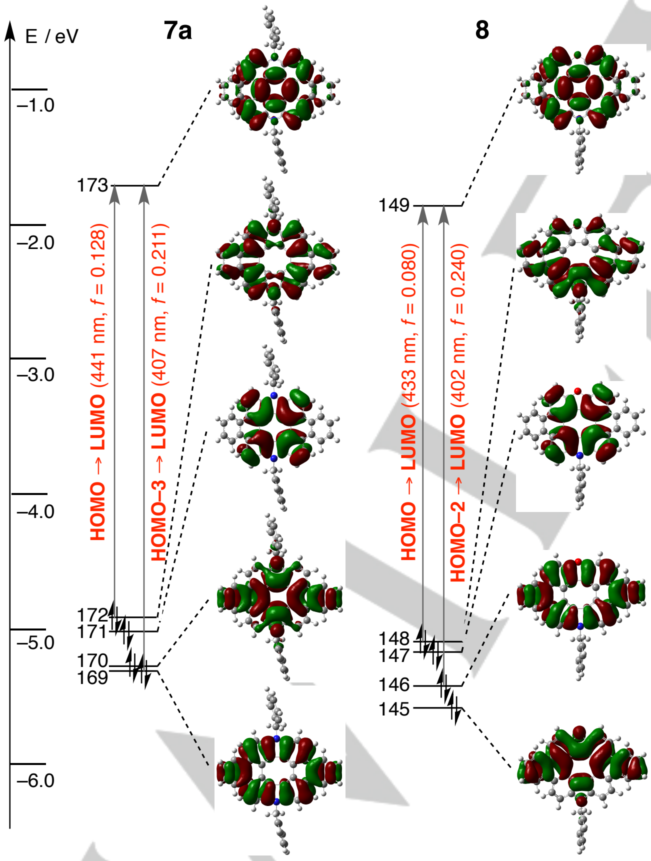

Figure 6. Molecular orbital diagrams of **7a** and **8** calculated at the B3LYP/6-31G* level.

Conclusion

In conclusion, double intramolecular oxidative aromatic coupling enables the transformation of substituted carbazoles into aza[7]helicenes **1a**–**c**, hetero[9]helicenes **1f**–**i**, triple helicene **3**, and azahepta[8]circulene **4**. DFT calculations suggested that the unexpected double rearrangement from **2e** to **3** proceeded via the arenium cation intermediate. These helical dyes showed CPL with the $|g_{lum}|$ in the range of 2.5 × 10^{-4}–3.5 × 10^{-3}. Furthermore, azahepta[8]circulene **4** was converted into diaza[8]circulenes **7a** and **7b** and azaoxa[8]circulene **8** via the double amination reaction. X-ray diffraction analysis of **7a** revealed the saddle-shaped diaza[8]circulene framework. In the present study, the X-ray crystal structure and solution-state properties of diheterole-based [8]circulenes have been reported for the first time. The short-step synthesis of azahelicenes and aza[8]circulenes in this work will be applicable to the synthesis of related helicenes and PAHs. Further investigations on the development of novel helicenes and circulenes are ongoing in our laboratory.

Deposition Numbers 2061453 (for **1c**), 2061454 (for **1h**), 2061455 (for **7a**), 2061456 (for **1b**), 2061457 (for **6**), 2061458 (for **3**) contain the supplementary crystallographic data for this paper. These data are provided free of charge by the joint Cambridge Crystallographic Data Centre and Fachinformationszentrum Karlsruhe Access Structures service www.ccdc.cam.ac.uk/structures.

Acknowledgements

This work was supported by JSPS KAKENHI Grant Number 18K05083. We thank Prof. Suga and Prof. Mitsudo (Okayama University) for CV measurements and Dr. K. Takaishi (Okayama University) for TD-DFT calculations.

Keywords: carbazoles • circularly polarized luminescence • circulenes • dyes • helicenes

[1] a) T. Hensel, N. N. Andersen, M. Plesner, M. Pittelkow, *Synlett* **2016**, *27*, 498; b) Y. Miyake, H. Shinokubo, *Chem. Commun.* **2020**, *56*, 15605.

[2] a) K. Yamamoto, T. Harada, Y. Okamoto, H. Chikamatsu, M. Nakazaki, Y. Kai, T. Nakao, M. Tanaka, S. Harada, N. Kasai, *J. Am. Chem. Soc.* **1988**, *110*, 3578; b) S. K. Pedersen, K. Eriksen, N. N. Karaush-Karmazin, B. Minaev, H. Ågren, G. V. Baryshnikov, M. Pittelkow, *Angew. Chem. Int. Ed.* **2020**, *59*, 5144; *Angew. Chem.* **2020**, *132*, 5182; c) S. K. Pedersen, K. Eriksen, H. Ågren, B. F. Minaev, N. N. Karaush-Karmazin, O. Hammerich, G. V. Baryshnikov, M. Pittelkow, *J. Am. Chem. Soc.* **2020**, *142*, 14058.

[3] a) C.-N. Feng, M.-Y. Kuo, Y.-T. Wu, *Angew. Chem. Int. Ed.* **2013**, *52*, 7791; *Angew. Chem.* **2013**, *125*, 7945; b) Y. Sakamoto, T. Suzuki, *J. Am. Chem. Soc.* **2013**, *135*, 14074; c) R. W. Miller, S. E. Averill, S. J. Van Wyck, A. C. Whalley, *J. Org. Chem.* **2016**, *81*, 12001; d) S. H. Pun, Y. Wang, M. Chu, C. K. Chan, Y. Li, Z. Liu, Q. Miao, *J. Am. Chem. Soc.* **2019**, *141*, 9680.

[4] a) C. B. Nielsen, T. Brock-Nannestad, P. Hammershøj, T. K. Reenberg, M. Schau-Magnussen, D. Trpcevski, T. Hensel, R. Salcedo, G. V. Baryshnikov, B. F. Minaev, M. Pittelkow, *Chem. Eur. J.* **2013**, *19*, 3898; b) T. Hensel, D. Trpcevski, C. Lind, R. Grosjean, P. Hammershøj, C. B. Nielsen, T. Brock-Nannestad, B. E. Nielsen, M. Schau-Magnussen, B. F. Minaev, G. V. Baryshnikov, M. Pittelkow, *Chem. Eur. J.* **2013**, *19*, 17097; c) F. Chen, Y. S. Hong, S. Shimizu, D. Kim, T. Tanaka, A. Osuka, *Angew. Chem. Int. Ed.* **2015**, *54*, 10639; *Angew. Chem.* **2015**, *127*, 10785; d) S.

Kato, Y. Serizawa, D. Sakamaki, S. Seki, Y. Miyake, H. Shinokubo, *Chem. Commun.* **2015**, *51*, 16944; e) Y. Nagata, S. Kato, Y. Miyake, H. Shinokubo, *Org. Lett.* **2017**, *19*, 2718; f) Y. Matsuo, F. Chen, K. Kise, T. Tanaka, A. Osuka, *Chem. Sci.* **2019**, *10*, 11006; g) H. Murase, Y. Nagata, S. Akahori, H. Shinokubo, Y. Miyake, *Chem. Asian J.* **2020**, *15*, 3873; h) B. Lousen, S. K. Pedersen, P. Bols, K. H. Hansen, M. R. Pedersen, O. Hammerich, S. Bondarchuk, B. Minaev, G. V. Baryshnikov, H. Ågren, M. Pittelkow, *Chem. Eur. J.* **2020**, *26*, 4935; i) Y. Matsuo, T. Tanaka, A. Osuka, *Chem. Eur. J.* **2020**, *26*, 8144.

[5] a) K. Y. Chernichenko, V. V. Sumerin, R. V. Shpanchenko, E. S. Balenkova, V. G. Nenajdenko, *Angew. Chem. Int. Ed.* **2006**, *45*, 7367; *Angew. Chem.* **2006**, *118*, 7527; b) A. Dadvand, F. Cicoira, K. Y. Chernichenko, E. S. Balenkova, R. M. Osuna, F. Rosei, V. G. Nenajdenko, D. F. Perepichka, *Chem. Commun.* **2008**, 5354; c) Y. Serizawa, S. Akahori, S. Kato, H. Sakai, T. Hasobe, Y. Miyake, H. Shinokubo, *Chem. Eur. J.* **2017**, *23*, 6948; d) S. Akahori, H. Sakai, T. Hasobe, H. Shinokubo, Y. Miyake, *Org. Lett.* **2018**, *20*, 304; e) L. Li, S. Zhao, B. Li, L. Xu, C. Li, J. Shi, H. O. Wang, *Org. Lett.* **2018**, *20*, 2181.

[6] K. Nakamura, Q.-Q. Li, O. Krejčí, A. S. Foster, K. Sun, S. Kawai, S. Ito, *J. Am. Chem. Soc.* **2020**, *142*, 11363.

[7] a) Y. Shen, C.-F. Chen, *Chem. Rev.* **2012**, *112*, 1463; b) W.-L. Zhao, M. Li, H.-Y. Lu, C.-F. Chen, *Chem. Commun.* **2019**, *55*, 13793; c) K. Dhbaibi, L. Favereau, J. Crassous, *Chem. Rev.* **2019**, *119*, 8846.

[8] a) S. D. Dreher, D. J. Weix, T. J. Katz, *J. Org. Chem.* **1999**, *64*, 3671; b) K. Nakano, Y. Hidehira, K. Takahashi, T. Hiyama, K. Nozaki, *Angew. Chem. Int. Ed.* **2005**, *44*, 7136; *Angew. Chem.* **2005**, *117*, 7298; c) G. M. Upadhyay, H. R. Talele, S. Sahoo, A. V. Bedekar, *Tetrahedron Lett.* **2014**, *55*, 5394; d) G. M. Upadhyay, A. V. Bedekar, *Tetrahedron* **2015**, *71*, 5644; e) G. M. Upadhyay, H. R. Talele, A. V. Bedekar, *J. Org. Chem.* **2016**, *81*, 7751; f) M. Krzeszewski, T. Kodama, E. M. Espinoza, V. I. Vullev, T. Kubo, D. T. Gryko, *Chem. Eur. J.* **2016**, *22*,16478; g) F. Chen, T. Tanaka, Y. S. Hong, T. Mori, D. Kim, A. Osuka, *Angew. Chem. Int. Ed.* **2017**, *56*, 14688; *Angew. Chem.* **2017**, *129*, 14880; h) K. Uematsu, K. Noguchi, K. Nakano, *Phys. Chem. Chem. Phys.* **2018**, *20*, 3286; i) G. M. Labrador, C. Besnard, T. Bürgi, A. I. Poblador-Bahamonde, J. Bosson, J. Lacour, *Chem. Sci.* **2019**, *10*, 7059; j) S. K. Pedersen, K. Eriksen, M. Pittelkow, *Angew. Chem. Int. Ed.* **2019**, *58*, 18419; *Angew. Chem.* **2019**, *131*, 18590; k) F. Saal, F. Zhang, M. Holzapfel, M. Stolte, E. Michail, M. Moos, A. Schmiedel, A.-M. Krause, C. Lambert, F. Würthner, P. Ravat, *J. Am. Chem. Soc.* **2020**, *142*, 21298.

[9] a) K. Goto, R. Yamaguchi, S. Hiroto, H. Ueno, T. Kawai, H. Shinokubo, *Angew. Chem. Int. Ed.* **2012**, *51*, 10333; *Angew. Chem.* **2012**, *124*, 10479; b) C. Shen, M. Srebro-Hooper, M. Jean, N. Vanthuyne, L. Toupet, J. A. G. Williams, A. R. Torres, A. J. Riives, G. Muller, J. Autschbach, J. Crassous, *Chem. Eur. J.* **2017**, *23*, 407; c) A. Ushiyama, S. Hiroto, J. Yuasa, T. Kawai, H. Shinokubo, *Org. Chem. Front.* **2017**, *4*, 664; d) T. Otani, A. Tsuyuki, T. Iwachi, S. Someya, K. Tateno, H. Kawai, T. Saito, K. S. Kanyiva, T. Shibata, *Angew. Chem. Int. Ed.* **2017**, *56*, 3906; *Angew. Chem.* **2017**, *129*, 3964; e) H. Nishimura, K. Tanaka, Y. Morisaki, Y. Chujo, A. Wakamiya, Y. Murata, *J. Org. Chem.* **2017**, *82*, 5242; f) Z. Domínguez, R. López-Rodríguez, E. Álvarez, S. Abbate, G. Longhi, U. Pischel, A. Ros, *Chem. Eur. J.* **2018**, *24*, 12660; g) J. Full, S. P. Panchal, J. Gςtz, A.-M. Krause, A. Nowak-Król, *Angew. Chem. Int. Ed.* **2021**, *60*, 4350; *Angew. Chem.* **2021**, *133*, 4396.

[10] a) K. Nakamura, S. Furumi, M. Takeuchi, T. Shibuya, K. Tanaka, *J. Am. Chem. Soc.* **2014**, *136*, 5555; b) T. Matsuno, Y. Koyama, S. Hiroto, J. Kumar, T. Kawai, H. Shinokubo, *Chem. Commun.* **2015**, *51*, 4607; c) Y. Uchida, T. Hirose, T. Nakashima, T. Kawai, K. Matsuda, *Org. Lett.* **2016**, *18*, 2118; d) H. Oyama, M. Akiyama, K. Nakano, M. Naito, K. Nobusawa, K. Nozaki, *Org. Lett.* **2016**, *18*, 3654; e) Y. Yamamoto, H. Sakai, J. Yuasa, Y. Araki, T. Wada, T. Sakanoue, T. Takenobu, T. Kawai, T. Hasobe, *Chem. Eur. J.* **2016**, *22*, 4263; f) K. Dhbaibi, L. Favereau, M. Srebro-Hooper, M. Jean, N. Vanthuyne, F. Zinna, B. Jamoussi, L. D. Bari, J. Autschbach, J. Crassous, *Chem. Sci.* **2018**, *9*, 735; g) Y. Nakakuki, T. Hirose, H. Sotome, H. Miyasaka, K. Matsuda, *J. Am. Chem. Soc.* **2018**, *140*, 4317; h) C. M. Cruz, S. Castro-Fernádez, E. Maçôas, J. M. Cuerva, A. G. Campaña, *Angew. Chem. Int. Ed.* **2018**, *57*, 14782; *Angew. Chem.* **2018**, *130*, 14998; i) H. Kubo, D. Shimizu, T. Hirose, K. Matsuda, *Org. Lett.* **2020**, *22*, 9276; j) Z. Qiu, S. Asako, Y. Hu, C.-W. Ju, T. Liu, L. Rondin, D. Schollmeyer, J.-S. Lauret, K. Müllen, A. Narita, *J. Am. Chem. Soc.* **2020**, *142*, 14814; k) Z. Qiu, C.-W. Ju, L. Frédéric, Y. Hu, D. Schollmeyer, G. Pieters, K. Müllen, A. Narita, *J. Am. Chem. Soc.* **2021**, *143*, 4661; l) G. Li, T. Matsuno, Y. Han, S. Wu, Y. Zou, Q. Jiang, H. Isobe, J. Wu, *Angew. Chem. Int. Ed.* **2021**, *60*, 10326; *Angew. Chem.* **2021**, *133*, 10414.

[11] a) C. Maeda, T. Todaka, T. Ema, *Org. Lett.* **2015**, *17*, 3090; b) C. Maeda, T. Todaka, T. Ueda, T. Ema, *Chem. Eur. J.* **2016**, *22*, 7508; c) C. Maeda, K. Nagahata, T. Ema, *Org. Biomol. Chem.* **2017**, *15*, 7783; d) C. Maeda, T. Todaka, T. Ueda, T. Ema, *Org. Biomol. Chem.* **2017**, *15*, 9283; e) C. Maeda, K. Nagahata, K. Takaishi, T. Ema, *Chem. Commun.* **2019**, *55*, 3136; f) C. Maeda, K. Suka, K. Nagahata, K. Takaishi, T. Ema, *Chem. Eur. J.* **2020**, *26*, 4261; g) C. Maeda, K. Nagahata, T. Shirakawa, T. Ema, *Angew. Chem. Int. Ed.* **2020**, *59*, 7813; *Angew. Chem.* **2020**, *132*, 7887; h) C. Maeda, S. Nomoto, K. Takaishi, T. Ema, *Chem. Eur. J.* **2020**, *26*, 13016.

[12] Hepta[8]circulene is defined as cyclooctatetraene with seven surrounding fused rings.[2a,21]

[13] Although intermolecular Scholl reactions sometimes take place,[22] the reaction in this work selectively produced intramolecular reaction products **1a**–**c** or **1f**–**h**.

[14] The spin density at the terminal benzene rings of the cation radical of methoxy-appended helicene was calculated to be higher than that of **1a** or **1b**, which might promote the concurrent C–C bond formation to produce **4** (Supporting Information).

[15] For examples of the formation of nonhexagonal rings via Scholl reactions, see: a) K. Kawasumi, Q. Zhang, Y. Segawa, L. T. Scott, K. Itami, *Nature Chem.* **2013**, *5*, 739; b) H.-W. Ip, C.-F. Ng, H.-F. Chow, D. Kuck, *J. Am. Chem. Soc.* **2016**, *138*, 13778; c) L. He, C.-F. Ng, Y. Li, Z. Liu, D. Kuck, H.-F. Chow, *Angew. Chem. Int. Ed.* **2018**, *57*, 13635; *Angew. Chem.* **2018**, *130*, 13823.

[16] For examples of a rearrangement during Scholl reactions, see: a) J. Liu, A. Narita, S. Osella, W. Zhang, D. Schollmeyer, D. Beljonne, X. Feng, K. Müllen, *J. Am. Chem. Soc.* **2016**, *138*, 2602; b) S. Nobusue, K. Fujita, Y. Tobe, *Org. Lett.* **2017**, *19*, 3227; c) X. Zhang, Z. Xu, W. Si, K. Oniwa, M. Bao, Y. Yamamoto, T. Jin, *Nat. Commun.* **2017**, *8*, 15073; d) M. Krzeszewski, K. Sahara, Y. M. Poronik, T. Kubo, D. T. Gryko, *Org. Lett.* **2018**, *20*, 1517.

[17] Coalescence was not observed from the ^{1}H NMR spectra of **1a** at 30–150 °C, suggesting that the racemization of the azahelicenes is strictly prohibited.

[18] The use of protonic acid such as MSA instead of $BF_3{\cdot}OEt_2$ also produced **3**, while chloranil/$BF_3{\cdot}OEt_2$ system was found to produce **3** in the highest yield. Although the initial catalytic proton source is unclear, a proton generated during the Scholl reaction might catalyze the arenium cation pathway.

[19] Because model compound (**R**) lacks another naphthylphenyl group, the possible repulsion between the two substituents was not included. If the repulsion is considered, the TS energy of **A1** to **A6** would be significantly higher, while that of **A1** to **A2** would not be strongly affected.

[20] BBr_3-mediated formation of furan rings to give tetraheterole-based [8]circulenes were reported by Tanaka[4f] and Pittelkow.[4h]

[21] a) C.-N. Feng, W.-C. Hsu, J.-Y. Li, Y.-T. Wu, *Chem. Eur. J.* **2016**, *22*, 9198; b) F. Chen, T. Tanaka, T. Mori, A. Osuka, *Chem. Eur. J.* **2018**, *24*, 7489.

[22] B. T. King, J. Kroulík, C. R. Robertson, P. Rempala, C. L. Hilton, J. D. Korinek, L. M. Gortari, *J. Org. Chem.* **2007**, *72*, 2279.

10.1002/chem.202102269

Entry for the Table of Contents

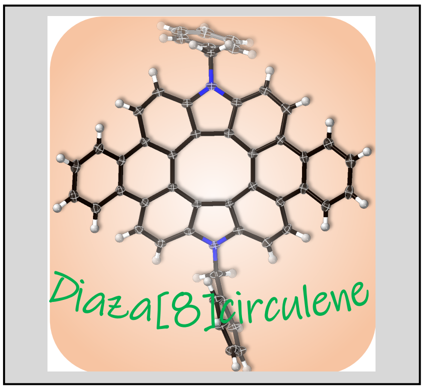

Intramolecular Scholl reaction of carbazole derivatives afforded highly strained azahelicenes and azahepta[8]circulene which was transformed into dibenzodiaza[8]circulenes. The diaza[8]circulene structure was characterized for the first time by X-ray diffraction analysis which revealed the saddle-shaped π-conjugated polyaromatics.